

Lead Salt Quantum Dots: the Limit of Strong Quantum Confinement

FRANK W. WISE

Department of Applied Physics, Cornell University,
Ithaca, New York 14853

Received March 23, 2000

ABSTRACT

Nanocrystals or quantum dots of the IV–VI semiconductors PbS, PbSe, and PbTe provide unique properties for investigating the effects of strong confinement on electrons and phonons. The degree of confinement of charge carriers can be many times stronger than in most II–VI and III–V semiconductors, and lead salt nanostructures may be the only materials in which the electronic energies are determined primarily by quantum confinement. This Account briefly reviews recent research on lead salt quantum dots.

Introduction

The properties of semiconductor nanocrystals or quantum dots (QDs) have received significant attention in the past decade. Following pioneering work by Efros and Ekimov,¹ Brus,² and Henglein,³ many II–VI and III–V materials have been prepared as QDs. Much progress has been achieved in the areas of synthesis, structural characterization, electronic and optical properties, and thermodynamics of semiconductor QDs. Overviews of the subject and recent research are listed in ref 4.

Many of the interesting and potentially useful properties of nanocrystals can be understood at the level of undergraduate quantum mechanics. When a particle (an electron in this case) is confined to a volume in space, two things happen: it acquires kinetic energy (referred to as confinement energy), and its energy spectrum becomes discrete. In a bulk semiconductor, the conduction electrons are free to move around in the solid, so their energy spectrum is almost continuous, and the density of allowed electron states per unit energy increases as the square-root of energy (Figure 1a). If one can synthesize a piece of the semiconductor so small that the electron “feels” confined, the continuous spectrum will become discrete and the energy gap will increase, as indicated in Figure 1b. What sets the size scale at which the electron feels confined? The crystallite must be comparable to the Bohr radius of the bound state of an electron and a hole. Such an electron–hole pair (called an exciton) is analogous to a hydrogen atom and can be thought of as the lowest excited electronic state of the bulk solid. An

Frank Wise received a B.S. degree in engineering physics from Princeton University (1980), an M.S. degree in electrical engineering from the University of California, Berkeley (1982), and a Ph.D. degree in applied physics from Cornell University (1989). From 1982 to 1984 he worked on advanced integrated circuit development at Bell Laboratories, Murray Hill, NJ. Since 1989 he has been in the Department of Applied Physics at Cornell.

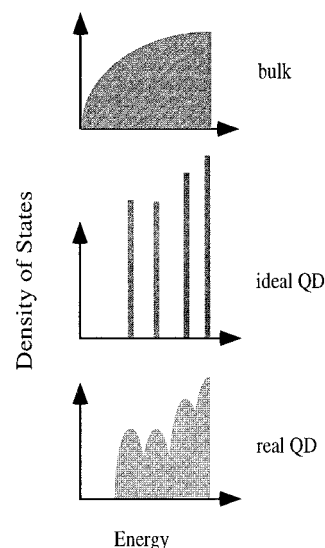


FIGURE 1. Density of electron states in bulk and size-quantized semiconductor. The optical absorption spectrum is roughly proportional to the density of states.

electron–hole pair in a QD is usually referred to as an exciton, even when the charge carriers are bound by the confining potential rather than the Coulomb interaction.

As Figure 1 illustrates, control of size allows us to engineer the optical properties of a semiconductor: strong absorption occurs at certain photon energies, at the expense of reduced absorption at other energies. Light always interacts with one electron–hole pair regardless of the size of the semiconductor, so the total or integrated absorption does not change. Ideally, the density of states becomes a series of delta functions (narrow spikes) in the QD, so those transitions must be very strong to conserve the integrated absorption. The strong transitions are the result of concentration of the optical transition strength into a few narrow energy intervals.

Ordinarily, the optical properties of a material do not depend on the intensity of the light, and as a result, light beams do not interact with each other. However, at high-enough intensities, materials become nonlinear—the light changes the material properties, which can then be sensed by a separate “probe” light beam or by the beam that changes the material itself. Optical nonlinearities can be used to implement switches based on light energy, which are potentially much faster than electrical switches, for example. Optical nonlinearities are generally strongest when the photon energy matches an optical transition in the solid; this property is referred to as resonant enhancement of the nonlinearity. With their strong absorptions, quantum dots offer the potential for strong resonantly enhanced optical nonlinearities and are thus candidate materials for applications such as optical switching and information processing.

This qualitative picture of the effects of quantum confinement in semiconductors is supported by rigorous theoretical calculations by Efros and Efros,¹ Brus,² and Schmitt-Rink et al.⁵ According to Schmitt-Rink et al., the

Table 1. Bohr Radii of Excitons in Representative Semiconductors

material	exciton Bohr radius (nm)
CuCl	1
CdSe	6
PbS	20
InAs	34
PbSe	46
InSb	54

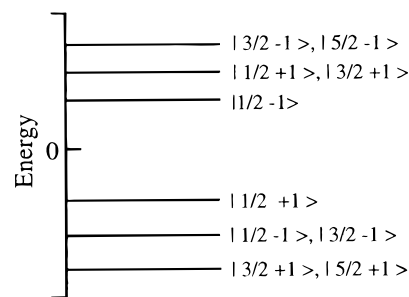
linear and resonant nonlinear optical properties will exhibit the greatest enhancement when the nanocrystal radius R is much smaller than the Bohr radius of the exciton (a_B) in the parent bulk material. This motivates the study of semiconductor QDs in the strong-confinement limit, where $R/a_B \ll 1$.

Large optical nonlinearities are expected as long as the QD transitions are not broadened excessively (Figure 1c). The magnitude and origin of the line-broadening are critical; any broadening opposes the spectral concentration of transition strength that comes from quantum confinement. The dominant intrinsic source of line broadening is expected to be coupling of the exciton to phonons—the optical transitions in QDs are inherently vibronic in nature, similar to those of a large molecule. This motivates studies of the strength of carrier–phonon interactions in nanocrystals.

Despite the effort that has gone into investigations of QDs in recent years, little experimental work has been done with samples that strongly confine both charge carriers. The difficulty of attaining the strong-confinement regime becomes clear when one considers the Bohr radii of excitons in semiconductors, which are typically ~ 10 nm or less. Some examples are given in Table 1.

For some phenomena the degree of localization of the individual charge carriers is relevant. If a_e and a_h are the Bohr radii of the electron and hole (imagine the charge carrier bound to a localized impurity, e.g.), then strong confinement occurs when $R \ll a_e, a_h$.¹ In semiconductors with large hole masses (i.e., most II–VI and III–V materials), it is impossible to achieve strong quantum confinement in this sense.

To investigate the strong-confinement limit, QDs of narrow-gap materials such as PbSe or InSb are desirable. Even in InSb, $a_h = 2$ nm, so strong confinement of the hole will be impossible. In contrast, $a_e = a_h = 23$ nm in PbSe. The similarly small electron and hole masses of the lead salts (PbS, PbSe, and PbTe) imply large confinement energies, split about equally between carriers. The electronic spectra of QDs of the lead salts are thus simple, with energy spacings that can be much larger than the energy gaps of the bulk materials (which are 0.2–0.4 eV). The generic form of the energy levels of PbS or PbSe QDs is shown in Figure 2. In contrast, the spectra of II–VI and III–V QDs are relatively congested due to closely spaced hole levels and are complicated significantly by valence-band mixing.^{6,7} Another potential advantage for studies of nanocrystal physics is the possibility of achieving strong quantum confinement of charge carriers without the properties being dominated by the surface of the QD. This

**FIGURE 2.** General form of the first few electron and hole energy levels of PbS or PbSe QDs. The states are labeled by the quantum numbers j (total angular momentum) and π (parity): $|j\pi\rangle$.**Table 2. Percentage of Atoms on the Surface of QDs of CdSe and PbSe with the Indicated Radii**

R/a_B	CdSe	PbSe
1	30%	5%
0.3	90%	15%
0.1		45%

is illustrated in Table 2. The influence of the surface on QD properties is complicated and remains controversial, so reducing this influence can be valuable in determining intrinsic QD properties. A final interesting feature of the lead salts is that they crystallize in the cubic sodium chloride structure, with every atom at a site of inversion symmetry. Structures with such high symmetry should be useful for assessing the intrinsic polarity of strongly size-quantized electron states.

The electronic structure has implications for the critical issue of exciton–phonon coupling in QDs, via the properties of the excited-state charge distribution. Although the coupling of electrons and holes to polar phonons is strong in the lead salts due to their ionicity, the exciton–phonon coupling should be small. In the strong-confinement limit the electron and hole have identical wave functions and can be thought of as lying on top of each other, canceling each other's coupling to the lattice. Thus, the coupling to polar phonons (which depends on the net charge inhomogeneity of the excited state) should vanish.⁵

The optical phonons of the bulk lead salts are highly dispersive, and the frequencies of the long-wavelength longitudinal and transverse optical phonons differ by a factor of 3. Using qualitative Fourier transform thinking, decreasing the size of a crystal corresponds to moving to larger wave vectors (shorter wavelengths) on a bulk phonon dispersion relation. This will produce an observable change in phonon frequency if the phonons are dispersive. The difference between ω_{LO} and ω_{TO} facilitates observation of the effects of coupling the bulk plane wave modes in the nanostructure. These properties contrast with the nearly flat and nearly degenerate optical phonon dispersion in II–VI and III–V semiconductors and make the lead salts valuable for studies of phonon confinement.

To summarize, lead salt QDs provide clear and unique opportunities for studying the properties of a strongly size-quantized electronic system. $R/a_B = 0.04$ is achieved with existing samples (examples are given below), and $R/a_B \approx 0.02$ is possible. For comparison, in commonly studied CdSe QDs the minimum value of $R/a_B \approx 0.16$. Most

exciton physics depends on the volume of the exciton, i.e., $(R/a_B)^3$, so the degree of confinement possible with the lead salts can be many times stronger than in II–VI and III–V materials. As one measure of this, the confinement energy can easily be *several times* the bulk energy gap in the lead salts, compared to about one-half the bulk energy gap in CdSe. The lead salts have potential advantages over other materials with regard to the nonlinear optical response due to the possibilities of achieving stronger confinement of the excitons and smaller intrinsic line widths due to reduced exciton–phonon coupling. Finally, QDs of narrow-gap materials should be relevant for applications: strong confinement can be achieved in a structure whose lowest-energy optical transition occurs at technologically important wavelengths in the near-infrared region of the electromagnetic spectrum.

Synthesis and Characterization

Early work on lead salt materials produced some evidence of size-quantized electronic states. Thin films of the lead salts were grown as early as 1960, and produced evidence of confinement in one dimension (i.e., a quantum well in today's language)⁸ as well as suggestions of three-dimensional confinement in crystallites of the polycrystalline films.^{9,10} The first intentionally synthesized IV–VI QDs exhibited increases in the energy gap that were attributed to quantum size effects.¹¹ However, structured absorption spectra were typically not observed, probably owing to a broad distribution of particle sizes. The synthesis of high-quality, monodisperse PbS QDs in poly(vinyl alcohol) (PVA) was reported in 1990.¹² Machol et al. duplicated that synthesis and succeeded in increasing the concentration of QDs as well as producing dense thin films of QDs.¹³ More recently, the controllable fabrication of PbS and PbSe QDs with diameters between 3 and 20 nm in glass hosts has been demonstrated.^{14–17} PbTe crystallites exhibiting exciton peaks blue-shifted from the bulk energy gap have been fabricated, but no structural characterization was reported.¹⁸

The PbS QDs in silicate glass¹⁴ offer excellent properties. The narrow size distribution ($\Delta R/R \approx 4\%$) is illustrated by the isolated exciton transitions visible in the room-temperature absorption spectrum shown in Figure 3. Even with excitation 1 eV above the lowest exciton, the luminescence spectrum emitted by these QDs is a single peak with a Stokes shift (reflecting primarily inhomogeneous broadening from the distribution of particle sizes) of 75 meV. Well-characterized dyes are not available as reference samples in the infrared, so an AlInAs/GaInAs quantum well laser structure was used to roughly estimate the luminescence quantum yield of ~ 0.1 at room temperature.¹⁹ For QD sizes between 5 and 10 nm, resonantly excited excitons decay with time constants of ~ 1 ns.²⁰ The initial relaxation of electrons in many QD samples occurs in ~ 10 ps and is thought to be due to fast trapping of one charge carrier or relaxation to a long-lived "dark" state²¹ from which recombination is spin-forbidden. The small luminescence Stokes shift, bright luminescence, and

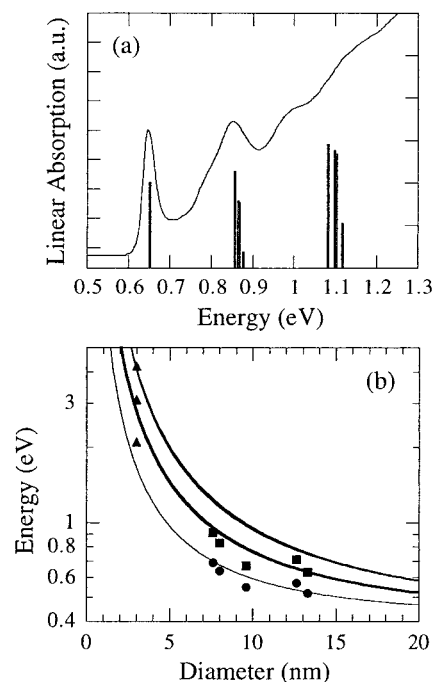


FIGURE 3. (a) Absorption spectrum and calculated transition strengths of 8.5-nm-diameter PbS QDs in oxide glass. (b) Measured and calculated exciton energies (plotted on a logarithmic scale) as a function of the size of PbS QDs. The dark lines indicate nearly degenerate transitions between the states indicated in Figure 2.

absence of rapid carrier trapping (in addition to the structural characterization) all indicate the high quality of these structures.

The synthesis and characterization of monodisperse PbSe QDs was reported by Lipovskii and co-workers.¹⁷ To our knowledge PbSe has the largest Bohr radius (46 nm) of any material synthesized as QDs in glass or colloid. QDs with diameters between 2 and 15 nm were produced, so the confinement is extreme in these QDs. A typical optical absorption spectrum is shown in Figure 4. The variation of the lowest exciton energy with size is also plotted along with the results of calculations to be described below.

Electronic States

A conceptually simple way to calculate the electron states of a QD is to impose spatial confinement on the electron states of the bulk material. In this effective-mass or envelope function approach,²² the wave functions are forced to zero at the boundary of the QD. Kang performed an envelope function calculation of the electronic structure of PbS and PbSe QDs.²³ The envelope function calculation provides the energy spectrum and wave functions (Figure 2), as well as dipole transition strengths and selection rules. The results of the calculation agree well with measured properties of PbS QDs down to 3 nm in diameter. Measured and calculated spectra are compared in Figure 3a as an example, and energy levels for several samples of PbS QDs are shown in Figure 3b. In the smallest (3-nm diameter) structures the exciton energy is 2 eV, which is *5 times* the bulk energy gap. The electronic

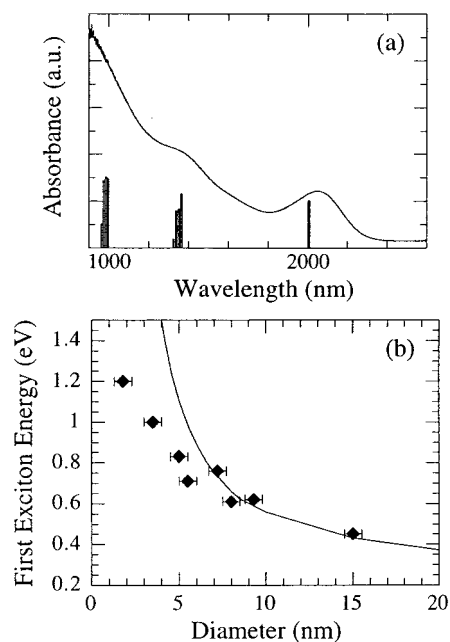


FIGURE 4. (a) Measured absorption spectrum (line) and calculated dipole transitions (bars) of 8.5-nm PbSe QDs. (b) Measured (symbols) and calculated (line) energies of the lowest exciton in PbSe QDs of varying size. Reproduced with permission from ref 17.

states of these structures are truly dominated by quantum confinement.

Kang's calculation was the first application of the envelope function approach to a narrow-gap material. This work demonstrates the utility of the multiband envelope function approach with the explicit inclusion of band nonparabolicity. Some features of the analysis differ from that of II–VI and III–VI materials. Two specific issues that are important for QD physics are the following:

(1) The transition dipole moment in lead salt QDs has a contribution from the envelope in addition to the usual dipole moment of the Bloch functions. This has consequences for the inter- and intraband transitions, and thus the one- and two-photon spectra.

(2) Fine structure arising from electron–hole Coulomb and exchange interactions has been a subject of much interest recently,²¹ and these many-body perturbations are included in Kang's analysis. The Coulomb interaction does not split the lowest exciton in lead salt QDs. The exchange interaction has an inter-unit-cell component that vanishes in other materials in addition to the intra-unit-cell component that is enhanced by quantum confinement. However, the magnitude of the exchange splitting is only ~ 10 meV in even the smallest lead salt QDs. This is smaller than in II–VI compounds.

The deviation between Kang's calculations and measurements of PbSe QDs with diameters between 3.5 and 7 nm (Figure 4b) is significant and may signal the breakdown of the effective mass approximation. The envelope function theory is not expected to be valid for the smallest (~ 2 nm) QDs, which are only a few lattice constants in diameter.

The envelope function calculation also fails to account for some transitions observed in PbS and PbSe QDs.

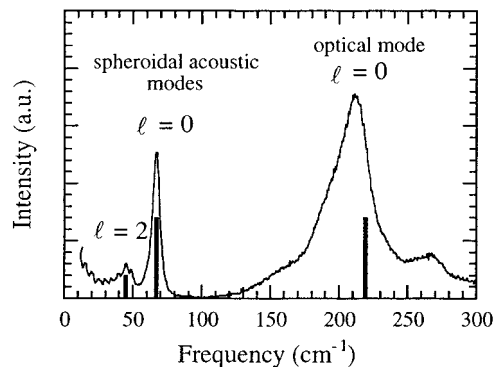


FIGURE 5. Raman spectrum of 3-nm PbS QDs. Vertical bars indicate calculated mode frequencies.

Examples are the features near 0.8 and 1.0 eV in Figure 3a. The constant-energy surfaces in k -space are slightly anisotropic in PbS and PbSe, and Kang treats the anisotropy as a perturbation to an otherwise isotropic model. A calculation following Kang's but treating the anisotropy exactly does indeed predict transitions that do not appear in the isotropic model.²⁴ Work is in progress to apply this approach to PbTe QDs,²⁵ which are interesting because the constant-energy surfaces of PbTe are extremely anisotropic.

Vibrational Modes

The vibrational modes of QDs have not received the extensive attention paid the electronic states. An accurate description of the vibrational modes of QDs is fundamentally important and is of course a prerequisite to understanding the electron–phonon coupling in QDs.

A rigorous theoretical treatment of the optical vibrational modes of semiconductor QDs was published in 1994,²⁶ and was followed by calculations of the Raman and infrared cross sections of these modes.²⁷ The theory accounts for both electromagnetic and mechanical boundary conditions at the surface of the QD, and the key overall prediction is that the modes in general have mixed transverse and longitudinal character as well as electromagnetic and mechanical nature.

The acoustic modes of QDs can often be modeled by assuming that the dot is an elastic continuum.²⁸ Application of spherical boundary conditions at the surface of the QD produces discrete torsional and spheroidal eigenmodes. The spheroidal modes with angular momenta $l = 0$ (a spherical breathing mode) and $l = 2$ (an ellipsoidal mode) should be Raman-active.²⁹

Krauss et al. extended the theoretical framework developed by Roca and co-workers to account for the unusual phonon dispersion of the lead salts, and calculated the vibrational frequencies for modes with angular momenta up to $l = 2$. The most interesting feature of this calculation is a band of infrared-active modes with frequencies around 100 cm^{-1} for $l = 1$. This band is far from the zone center frequencies $\omega_{\text{TO}} = 65 \text{ cm}^{-1}$ and $\omega_{\text{LO}} = 210 \text{ cm}^{-1}$.

Krauss and co-workers then measured the Raman scattering (Figure 5) and far-infrared absorption spectra

of PbS QDs. The results are consistent with the theoretical predictions and cannot be accounted for by prior models. These measurements thus confirm the influence of electrostatic and mechanical boundary conditions on the vibrational modes of QDs and can be considered an observation of the true optical modes of a semiconductor QD.³⁰

Electron–Phonon Coupling

In the strong-confinement limit, the size-quantized electron and hole ideally have identical wave functions, and the coupling to polar phonons should vanish. Coupling to acoustic phonons occurs through deformation potential and piezoelectric interactions. The sodium chloride crystal structure of the lead salts is centrosymmetric and thus not piezoelectric, so the deformation potential coupling is isolated. QDs of the lead salts are thus well-suited to test theoretical predictions of the vibronic nature of the excited states and the homogeneous line shape.

Once the electronic wave functions and vibrational modes were known, they could be used to calculate the coupling of excitons to optical modes. For all sizes, the coupling strength (in units of the energy of the vibrational mode with $l = 0$) $S < 10^{-4}$. In terms of a shifted harmonic oscillators model (as commonly used to describe dye molecules, e.g.), S can be thought of as the mean number of vibrational quanta involved in an optical transition.

Experimentally, the exciton–phonon coupling in QDs has traditionally been inferred from overtones in the Raman spectrum.³¹ Krauss measured the overtone spectrum of 3-nm PbS QDs in polymer host and obtained the coupling strength $S \approx 0.7$ for the dominant optical mode with $l = 0$.³² This value is 4 orders of magnitude larger than that calculated from the intrinsic electronic states of the QD and would imply that one charge carrier is highly localized in the QD. What is the origin of this huge discrepancy? Rapid (~ 10 ps) trapping of photoexcited charge carriers is observed with PbS QDs in polymer hosts.³³ Trapped charge builds up on the QDs during the steady-state Raman measurements, producing local electric fields. Such fields could easily polarize the exciton and produce the apparently large coupling to optical modes. A correct measurement of the coupling to polar phonons in these samples would therefore have to be made before appreciable decay of the photoexcited exciton occurs, i.e., on the subpicosecond time scale.

Exciton–phonon couplings can be obtained from a three-pulse photon echo (3PPE) experiment,³⁴ which allows determination of the coupling on the femtosecond time scale. Krauss measured the 3PPE signal from excitons in PbS QDs using 40-fs pulses. A typical signal, which is proportional to the electronic polarization, is shown in Figure 6a along with a theoretical fit. The polarization is modulated at the acoustic phonon frequency (70 cm^{-1}), with only a small component at the optical phonon frequency (215 cm^{-1}). The best-fit exciton–phonon couplings are $S_{\text{acoustic}} = 0.1$ and $S_{\text{optical}} = 0.01$. The modulation is even clearer in the saturated-absorption signal (Figure

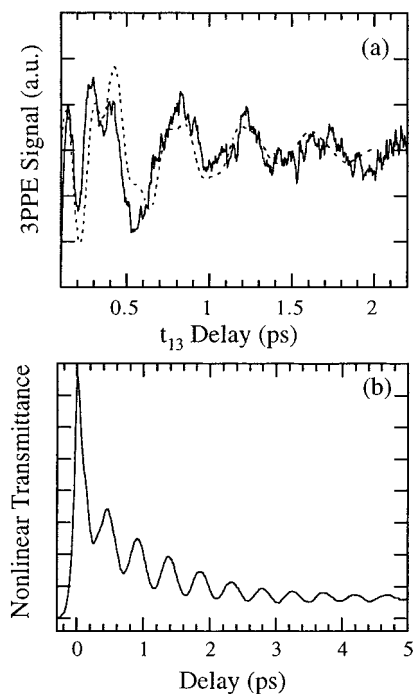


FIGURE 6. (a) Three-pulse photon echo signal (solid line) from 3-nm PbS QDs, along with theoretical fit (dashed). (b) Saturated-absorption signal. Reproduced with permission from ref 33.

6b), which monitors exciton population rather than polarization. The relative strengths of the optical and acoustic modes obtained by Fourier transforming the data of Figure 6b agree with those obtained from the 3PPE experiment. Calculation of the acoustic phonon coupling also predicts $S_{\text{acoustic}} \sim 0.1$.

These experiments lead to several conclusions:³³

- (1) Steady-state Raman measurement can overestimate the coupling to optical phonons by a factor of ~ 100 in QDs of narrow-gap materials.
- (2) The actual coupling to optical phonons is very small ($S_{\text{optical}} = 0.01$) due to net charge neutrality and is at least 10 times smaller than values obtained for QDs in other material systems.
- (3) The coupling to acoustic modes is larger than the coupling to optical modes.

The last two conclusions are consistent with the original theoretical predictions of Schmitt-Rink et al. for a QD in the limit of strong quantum confinement.⁵ Lead salts appear to be the only material system for which this is true.

Temperature Dependence of the Energy Gap

An interesting and illustrative consequence of the electronic and vibrational properties discussed above is the variation of the QD energy levels with temperature. For virtually all semiconductors, the temperature dependence of the energy gap is well-known experimentally. In bulk materials the temperature coefficient of the energy gap dE_g/dT has contributions from lattice thermal expansion and electron–phonon interactions. In the limit of a narrow energy band, theoretical analysis of dE_g/dT pro-

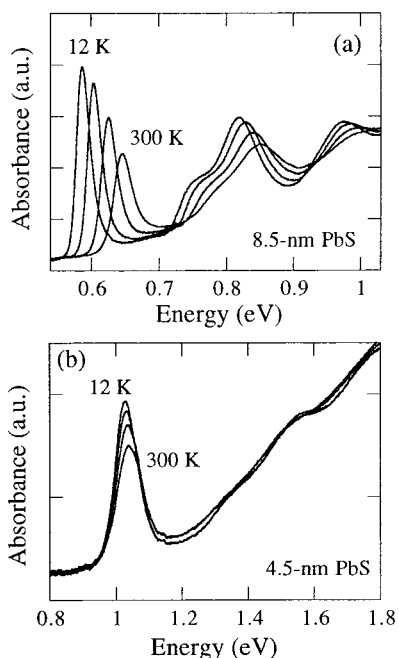


FIGURE 7. Absorption spectra of 8.5-nm (a) and 4.5-nm (b) PbS QDs recorded at 12, 100, 200, and 300 K. Adapted from ref 37.

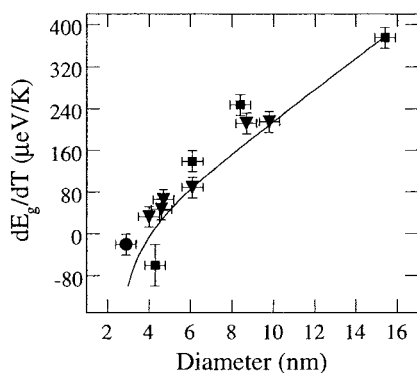


FIGURE 8. dE_g/dT for PbS QDs. Symbols are experimental values, and the line is the result of calculations. Adapted from ref 37.

duces an energy level independent of temperature, as expected for an isolated atom.³⁵ In QDs, we define the energy gap E_g as the energy of the lowest exciton transition. Studies generally report that the gap depends on temperature similarly to the energy gap of the bulk material.³⁶

Olkhovets and co-workers studied PbS QDs with diameter between 3 and 16 nm in glass and polymer hosts.³⁷ $a_B = 20$ nm in PbS, so the samples span the range from nearly bulk material to the strong-confinement limit. The exciton energies are determined from peaks in the optical absorption spectra measured at temperatures from 12 to 300 K. Typical experimental data are shown in Figure 7, and it is immediately evident that the spectra of smaller QDs are almost independent of temperature. The measured values of dE_g/dT are plotted versus QD size in Figure 8. dE_g/dT approaches the bulk value (~ 500 $\mu\text{eV/K}$) in the largest QDs and is nearly zero for the smallest QDs. The same trend is found with PbSe QDs. These are the first observations that the temperature coefficient of the energy

gap depends strongly on the size of a semiconductor and is nearly zero in the smallest structures.

The dominant contributions to the temperature variation of the energy gap of a QD come from the lattice dilation and electron–phonon coupling. A qualitative explanation of the observed size-dependence of dE_g/dT will be given here; quantitative details that produce the calculated line in Figure 8 can be found in ref 37. The effects of lattice thermal expansion diminish as the size of the structure decreases because the QD energy levels are determined more by the size of the structure rather than by the lattice constant. The effects of electron–phonon coupling on the energy levels can be calculated with perturbation theory. The energy denominators that appear in such a treatment lead to the well-known conclusion that coupling to nearby energy levels gives the greatest influence on a given level. The contribution to dE_g/dT from electron–phonon coupling decreases with decreasing size simply because the spacing between the quantum-confined energy levels (i.e., the denominator) increases. The fact that the energy gap becomes independent of temperature in the smallest QDs can therefore ultimately be understood as a consequence of strong quantum confinement. In QDs of II–VI and III–V materials, the intraband energy differences do not approach the bulk energy gap. As a result, dE_g/dT is similar to the bulk value.

Future Directions

All of the studies described here indicate that lead salt QDs should have extremely narrow spectral lines. This homogeneous or single-particle line width is not observed because of the inhomogeneous broadening that arises from the distribution in particle sizes. Optical spectroscopic techniques are available for determining the homogeneous line width under inhomogeneous broadening, but it would probably be more decisive to measure the spectra directly in single-particle experiments. Very narrow (μeV) excitation and luminescence lines have been observed from single QDs,³⁸ and it would be interesting to do similar experiments with the lead salts.

With regard to optical applications, the inhomogeneous broadening in ensemble samples and the difficulty of producing material with high concentration of QDs significantly reduce the effectiveness of QDs. It should also be pointed out that even the narrow spectral lines observed in single-QD experiments tend to move with time;³⁸ this “spectral diffusion” is another source of effective line broadening. Applications such as optical switching motivate the development of materials with large optical nonlinearities. Kang and Krauss have measured ultrafast absorption saturation (one manifestation of optical nonlinearity) in PbS and PbSe QDs, but only at very high fluence (~ 0.1 mJ/cm^2).³⁹ One of the “holy grails” of QD science is the development of a laser with a QD active medium. A currently debated issue that arises in the context of laser development is whether charge carriers injected into higher excited states of a QD will be

able to relax efficiently to the lowest excited state prior to recombination. In an ideal QD, relaxation by phonon emission is generally impossible except in the (rare) case where the phonon energy matches the energy-level spacing. The resulting "phonon bottleneck" to laser operation has not been observed yet, evidently owing to the existence of parallel relaxation channels in real QDs. Such channels probably involve the surface or defect states in many samples, although recent studies indicate that electron-hole interactions offer a parallel channel for electron relaxation.⁴⁰ Lead salt QDs should be good candidates for studying the intrinsic decay paths for electrons in QDs. Although inhomogeneous broadening is detrimental to most optical applications because it counters the effects of quantum confinement, it is interesting to note that a broad distribution of energies may be exploited to construct a broad-band optical amplifier for telecommunications.⁴¹ Emitters or detectors of light that do not depend on temperature could certainly be beneficial to some applications, and these are possible with lead salt QDs. A number of applications are envisioned for arrays of semiconductor QDs. These would allow combining the properties of QDs with photonic band-gap effects,⁴² as well as for collective or cooperative nonlinear effects based on interference. It is therefore quite exciting that the growth of arrays of PbSe QDs was demonstrated recently.⁴³ As a final example, in the past two years workers have demonstrated that semiconductor QDs can be used as fluorescent biological labels, with advantages over currently employed dye molecules.⁴⁴

Scientific studies as well as applications of QDs are all currently limited to some extent by the availability of appropriate samples. The past decade has seen major efforts aimed at developing the growth of II-VI and III-V QDs. By comparison, little has been done with IV-VI materials. With any effort in this area, it is reasonable to expect that IV-VI QDs will make major contributions to QD science and technology.

Conclusions

IV-VI semiconductors such as PbS and PbSe provide access to the limit of strong quantum confinement and are well-suited to the investigation of the properties of a size-quantized system. The electronic and vibrational spectra of lead salt QDs are relatively simple and sparse. Some of the features of lead salt QDs are relevant to applications in optoelectronics, telecommunications, and biophysics.

The author thanks all the students and collaborators who contributed to the work described here and acknowledges numerous stimulating discussions with A. L. Efros, N. Borrelli, and E. Lifshitz. This work was supported by the National Science Foundation under Grant DMR-9321259.

References

- (1) Efros, A. L.; Efros, A. L. Interband Absorption of Light in a Semiconductor Sphere. *Sov. Phys. Semicond.* **1982**, *16*, 772-774.
- Ekimov, A. I.; Efros, A. L.; Onushchenko, A. A. Quantum Size Effect in Semiconductor Microcrystals. *Solid State Commun.* **1985**, *56*, 921-924.

- (2) Brus, L. E. Electron-Electron and Electron-Hole Interactions in Small Semiconductor Crystallites: The Size Dependence of the Lowest Excited Electronic State. *J. Chem. Phys.* **1984**, *80*, 4403-4407.
- (3) See, for example, Weller, H.; Koch, U.; Gutierrez, M.; Henglein, A. Photochemistry of Colloidal Semiconductors. *Ber. Bunsenges. Phys. Chem.* **1984**, *88*, 649-655.
- (4) Banyai, L.; Koch, S. *Semiconductor Quantum Dots*; World Scientific: Singapore, 1993. For recent reviews see the following: Alivisatos, A. P. Semiconductor Clusters, Nanocrystals, and Quantum Dots. *Science* **1996**, *271*, 933-937. Nanoscale Materials Special Issue. *Acc. Chem. Res.* **1999**, *32*, 387-454.
- (5) Schmitt-Rink, S.; Miller, D. A. B.; Chemla, D. S. Theory of the Linear and Nonlinear Optical Properties of Semiconductor Microcrystallites. *Phys. Rev. B* **1987**, *35*, 8113-8124.
- (6) Ekimov, A. I.; Hache, F.; Schanne-Klein, M. C.; Ricard, D.; Flytzanis, C.; Kudryavtsev, I. A.; Yazeva, T. V.; Rodina, A. V.; Efros, A. L. Absorption and Intensity-Dependent Photoluminescence Measurements on CdSe Quantum Dots—Assignment of the 1st Electronic Transitions. *J. Opt. Soc. Am. B* **1993**, *10*, 100-107.
- (7) Norris, D. J.; Sacra, A.; Murray, C. B.; Bawendi, M. G. Measurement of the Size-Dependent Hole Spectrum in CdSe Quantum Dots. *Phys. Rev. Lett.* **1994**, *72*, 2612-2615.
- (8) Abou El Ela, A. H. The Absorption Band Edge of Lead Telluride Films Under Quantum Size Effect. *Rev. Phys. Appl.* **1975**, *10*, 105-108.
- (9) Lawson, W. D.; Smith, F. A.; Young, A. S. Influence of Crystal Size on the Spectral Response of Evaporated PbTe and PbSe Photo Cells. *J. Electrochem. Soc.* **1960**, *107*, 206-210.
- (10) Dadarlat, D.; Candea, R. M.; Thicu, R.; Biro, L. P.; Zasavitskii, I. I.; Valeiko, M. V.; Shotov, A. P. Size Effects in Polycrystalline PbSe Films Obtained by Chemical Deposition. *Phys. Stat. Sol. A* **1988**, *108*, 637-641.
- (11) Nozik, A. J.; Williams, F.; Nenadovic, M. I.; Rajh, T.; Micic, O. I. Size Quantization in Small Semiconductor Particles. *J. Phys. Chem.* **1985**, *89*, 397-400. Brus, L. E. Electronic Wave Functions in Semiconductor Clusters: Experiment and Theory. *J. Phys. Chem.* **1986**, *90*, 2555-2561. Wang, Y.; Nedeljkovic, J. M.; Nenadovic, M. I.; Micic, O. I. Blue Shift of Band Edge Seen in PbSe Colloids. *J. Phys. Chem.* **1986**, *90*, 12-13. Suna, A.; Mahler, W.; Kasowski, R. PbS in Polymers: From Molecules to Bulk Solids. *J. Chem. Phys.* **1987**, *87*, 7315-7317. Chang, A. C.; Pfeiffer, W. F.; Guillaume, B.; Baral, S.; Fendler, J. H. Preparation and Characterization of Selenide Semiconductor Particles in Surfactant Vesicles. *J. Chem. Phys.* **1990**, *94*, 4284-4289. Gorer, S.; Albu-Yaron, A.; Hodes, G. Quantum-Size Effects in Chemically Deposited, Nanocrystalline Lead Selenide Films. *J. Phys. Chem.* **1995**, *99*, 16442-16444.
- (12) Nenadovic, M. T.; Comor, M. I.; Vasic, V.; Micic, O. I. Transient Bleaching Of Small PbS Colloids—Influence Of Surface Properties. *J. Phys. Chem.* **1990**, *94*, 6390-6394.
- (13) Machol, J. L.; Wise, F. W.; Patel, R. C.; Tanner, D. B. Vibronic Quantum Beats in PbS Microcrystallites. *Phys. Rev. B* **1993**, *48*, 2819-2821.
- (14) Borrelli, N. F.; Smith, D. W. Quantum Confinement of PbS Microcrystals in Glass. *J. Non-Cryst. Sol.* **1994**, *180*, 25-31.
- (15) Lipovskii, A. A.; Kolobkova, E. V.; Olkhovets, A.; Petrikov, V. D.; Wise, F. Synthesis of Monodisperse PbS Quantum Dots in Phosphate Glass. *Physica E* **1999**, *5*, 157-160.
- (16) Lifshitz, E.; Sirota, M.; Porteanu, H. Continuous and Time-Resolved Photoluminescence Study of Lead Sulfide Nanocrystals, Embedded in Polymer Film. *J. Cryst. Growth* **1999**, *196*, 126-134.
- (17) Lipovskii, A.; Kolobkova, E.; Petrikov, V.; Kang, I.; Olkhovets, A.; Krauss, T.; Thomas, M.; Silcox, J.; Wise, F.; Shen, Q.; Kycia, S. Synthesis and Characterization of PbSe Quantum Dots in Phosphate Glass. *Appl. Phys. Lett.* **1997**, *71*, 3406-3408.
- (18) Reynoso, V. C. S.; de Paula, A. M.; Cuevas, R. F.; Medeiros Neto, J. A.; Alves, O. L.; Cesar, C. L.; Barbosa, L. C. PbTe Quantum-Dot Doped Glasses With Absorption-Edge in the 1.5- μm Wavelength Region. *Electron. Lett.* **1995**, *31*, 1013-1015.
- (19) Hsu, R. C. M.S. Thesis, Cornell University, Ithaca, NY, 2000.
- (20) Kang, I.; Krauss, T. D. Unpublished.
- (21) Nirmal, M.; Norris, D. J.; Kuno, M.; Bawendi, M. G.; Efros, A. L.; Rosen, M. Observation of the Dark Exciton in Cdse Quantum Dots. *Phys. Rev. Lett.* **1995**, *75*, 3728-3731.
- (22) Efros, A. L. Luminescence Polarization of CdSe Microcrystals. *Phys. Rev. B* **1992**, *46*, 7448-7458. Efros, A. L.; Rodina, A. V. Band-Edge Absorption and Luminescence of Nonspherical Nanometer-Size Crystals. *Phys. Rev. B* **1993**, *47*, 10005-10007.
- (23) Kang, I.; Wise, F. W. Electronic Structure and Optical Properties of PbS and PbSe Quantum Dots. *J. Opt. Soc. Am. B* **1997**, *14*, 1632-1646.

- (24) Andreev, A. D.; Lipovskii, A. A. Anisotropy-Induced Optical Transitions in PbS and PbSe Spherical Quantum Dots. *Phys. Rev. B* **1999**, *59*, 15402–15404.
- (25) Andreev, A. D.; Kang, I.; Wise, F. W. Unpublished.
- (26) Roca, E.; Trallero-Giner, C.; Cardona, M. Polar Optical Vibrational Modes in Quantum Dots. *Phys. Rev. B* **1994**, *49*, 13704–13711.
- (27) Chamberlain, M. P.; Trallero-Giner, C.; Cardona, M. Theory of One-Phonon Raman Scattering in Semiconductor Microcrystallites. *Phys. Rev. B* **1995**, *51*, 1680–1693.
- (28) Lamb, H. On the Vibrations of an Elastic Sphere. *Proc. London Math. Soc.* **1882**, *13*, 189–198.
- (29) Duval, E. Far-Infrared and Raman Vibrational Transitions Of A Solid Sphere—Selection Rules. *Phys. Rev. B* **1992**, *46*, 5795–5798.
- (30) Krauss, T. D.; Wise, F. W.; Tanner, D. B. Observation of Coupled Vibrational Modes of a Semiconductor Nanocrystal. *Phys. Rev. Lett.* **1996**, *76*, 1376–1379.
- (31) For example, see: Alivisatos, A. P.; Harris, T. D.; Carroll, P. J.; Steigerwald, M. L.; Brus, L. E. Electron-Vibration Coupling in Semiconductor Clusters Studied by Resonance Raman-Spectroscopy. *J. Chem. Phys.* **1989**, *90*, 3463–3470.
- (32) Krauss, T. D.; Wise, F. W. Raman-Scattering Study of Exciton–Phonon Coupling in PbS Nanocrystals. *Phys. Rev. B* **1997**, *55*, 9860–9865.
- (33) Krauss, T. D.; Wise, F. W. Coherent Acoustic Phonons in a Semiconductor Quantum Dot. *Phys. Rev. Lett.* **1997**, *79*, 5102–5105.
- (34) Mukamel, S. *Principles of Nonlinear Optical Spectroscopy*; Oxford University Press: New York, 1995.
- (35) Allen, P.; Heine, V.; Theory of the Temperature Dependence of Electronic Band Structures. *J. Phys. C: Solid State Phys.* **1976**, *9*, 2305–2312.
- (36) For example, Vossmeier, T.; Katsikas, L.; Giersig, M.; Popovic, I. G.; Diesner, K.; Chemseddine, A.; Eychmuller, A.; Weller, H. CdS Nanoclusters: Synthesis, Characterization, Size-Dependent Oscillator Strength, Temperature Shift Of The Excitonic Transition Energy, and Reversible Absorbance Shift. *J. Phys. Chem.* **1994**, *98*, 7665–7673.
- (37) Olkhovets, A.; Hsu, R. C.; Lipovskii, A.; Wise, F. W. Size-Dependent Temperature Variation of the Energy Gap in Lead-Salt Quantum Dots. *Phys. Rev. Lett.* **1998**, *81*, 3539–3542.
- (38) Marzin, J. Y.; Gerard, J. M.; Izreal, A.; Barrier, D.; Bastard, G. Photoluminescence of Single InAs Quantum Dots Obtained by Self-Organized Growth On GaAs. *Phys. Rev. Lett.* **1994**, *73*, 716–719. Empedocles, S. A.; Norris, D. J.; Bawendi, M. G. Photoluminescence Spectroscopy of Single CdSe Nanocrystallite Quantum Dots. *Phys. Rev. Lett.* **1996**, *77*, 3873–3876.
- (39) Kang, I.; Krauss, T. D.; Wise, F. W. Unpublished.
- (40) Klimov, V. I.; Mikhailovsky, A. A.; McBranch, D. W.; Leatherdale, C. A.; Bawendi, M. G. Mechanisms for Intraband Energy Relaxation in Semiconductor Quantum Dots: The Role of Electron–Hole Interactions. *Phys. Rev. B* **2000**, *61*, 13349–13352.
- (41) Efros, Al.; Khurgin, J. Personal communication.
- (42) Joannopoulos, J. D.; Meade, R. D.; Winn, J. N. *Photonic Crystals: Molding the Flow of Light*; Princeton University Press: Princeton, NJ, 1995.
- (43) Springholz, G.; Holy, V.; Pinczolit, M.; Bauer, G. Self-Organized Growth of Three-Dimensional Quantum-Dot Crystals with FCC–Like Stacking and a Tunable Lattice Constant. *Science* **1998**, *282*, 734–737.
- (44) Bruchez, M.; Moronne, M.; Gin, P.; Weiss, S.; Alivisatos, A. P. Semiconductor Nanocrystals as Fluorescent Biological Labels. *Science* **1998**, *281*, 2013–2016. Chan, W. C. W.; Nie, S. Quantum Dot Bioconjugates for Ultrasensitive Nonisotopic Detection. *Science* **1998**, *281*, 2016–2019.

AR970220Q